Silicon (2019) 11:1809–1816
https://doi.org/10.1007/s12633-018-9998-6

ORIGINAL PAPER

The Chemistry of Allanite – Britholite Single Crystal in Alkaline Volcanic Rocks, from Gabal Umm Shaghir Area, Central Eastern Desert, Egypts

B. N. A. Shalaby[1] · A. I. M. Ismail[1] · A. K. A. Salem[1]

Received: 26 July 2018 / Accepted: 9 October 2018 / Published online: 25 October 2018

Abstract

The present study deals with the mineral chemistry and genesis of two rare earth elements bearing silicate minerals, namely; allanite and britholite, co-existing in a single crystal, encountered in quartz trachyte dyke, considered to be an offshoot from Gabal Umm Shaghir trachytic plug, central Eastern Desert of Egypt. The size of present allanite-britholite crystal is about 0.25 mm in length and 0.10 mm in width. The allanite phase occupies the main bulk of the crystal, while the britholite phase, exits in the form of transversal spine-shaped lamellae. The mineral chemistry and the genesis of the present allanite - britholite phases are discussed based on 10 scanning electron microprobe point analyses. The present study also discuses, through elemental mapping, the distribution and concentration of selected 9 elements; Si, Fe, Mg, Al, Na, Ca, P, La and Ce, and their frequencies between different mineral phases. The average structural formula of present allanite based on 12.5 (O^{2-}) and 8 cations is: $(Ca^{2+})_{1.00}$ $(Ce^{3+}_{0.34}, La^{3+}_{0.19}, Nd^{3+}_{0.14}, Sm^{3+}_{0.02}, Y^{3+}_{0.11}, Ca^{2+}_{0.25})_{1.05}$ $(Mg^{2+}_{0.07}, Fe^{2+}_{0.69}, Fe^{3+}_{0.19})_{0.95}$ $(Ti^{4+}_{0.02}, Fe^{3+}_{0.13}, Al^{3+}_{0.85})_{1.00}$ $(Al^{3+})_{1.00}$ $(Si^{4+})_{2.99}$ $(O^{2-})_{12.5}$. The average structural formula of present britholite based on 12.5 (O^{2-}) and 8 cations is: $(Ca^{2+}_{1.73}, K^{+}_{0.05,}$ $Mg^{2+}_{0.10}, Fe^{2+}_{0.22}, Ti^{4+}_{0.01,}$ $Al^{3+}_{0.14,}$ $La^{3+}_{0.50}, Ce^{3+}_{1.19}, Nd^{3+}_{0.44}, Sm^{3+}_{0.10}, Y^{3+}_{0.50,}$ $Th^{4+}_{0.01})_{5.00}$ $(Al^{3+}_{0.12}, P^{5+}_{0.39}, Si^{4+}_{2.49})_{3.00}$ $(O^{2})_{12.5}$. The present study concluded that, the coexistence of britholite - allanite mineral phases were resulted from rare earth elements (REEs) + P enriched hydrothermal solutions, undergone percolation and attacking the allanite crystal along cleavage planes. The reaction processes involved, essentially, substitution of P_2O_5 and $REEs_2O_3$ for Al_2O_3 and SiO_2.

Keywords Allanite · Britholite · Rare earth elements · Alkaline rocks · Trachyte

1 Introduction

Allanite, $Ca(LREEs)Al_2Fe(SiO_4)(Si_2O_7)O(OH)$,is a subgroup of monoclinic minerals, originally used to describe LREEs-bearing members of the epidote group. The allanite subgroup, $A_2M_3Si_3O_{12}(OH)$, is derived from clinozoisite through homovalent substitutions and single coupled heterovalent substitution ; A_2:$REEs^{3+}$ + M_3: M^{2+} A_2:Ca^{2+} + M_3:M^{3+}. Accordingly, the key sites valences are: A_1 = M^{2+}, A_2 = M^{3+}, M_1 = M^{3+}, M_2 = M^{3+}, M_3 = M^{2+}, O_4 = O^{2-}, O_{10} = $(OH)^{-}$. Armbruster et al. [1]. Allanite" subgroup is further classified into allanite-(La), allanite-(Ce), and allanite-(Y), depending on the dominant lanthanon [2, 3].

Britholite $(Ca,LREEs,Y)_5(SiO_4,PO_4)_3(F,OH)$, is described as hexagonal mineral [4], and is considered by IMA as a group of minerals belonging to apatite super group [5]. It represents an isomorphous series with apatite, $Ca_5(PO_4)_3(F,Cl,OH)$, the common substitutions occur between Si^{4+} and $REEs^{3+}$for P^{4+} and Ca^{2+} [6]. Britholite is usually found associated with allanite, apatite, and fluorite in alkaline intrusions and granitic pegmatitites as a result of hydrothermal alteration.

Allanite, in Egypt, was encountered in many areas in the Eastern Desert, among them could be mentioned; pegmatitic dykes and veins at Wadi El Gemal area [7] and Gabal El Urf area [8], uraniferous pegmatites at Naslet Marufa area [9], and peraluminous leucocratic granite at Gabal Um Darag El Ahmer and Gabal Um Maiat Abu Ghaliqa areas [10].

The present area is located to the southwest of Qusseir City, Red Sea coast, between latitudes 25°58'17" and 26°04'54" N and longitudes 33°54'04" and 33°59'34" E.

✉ A. I. M. Ismail
aliism13@hotmail.com

[1] Geological Sciences Department, National Research Centre, P.O. 12622, 33 El Bohooth St. Dokki, Giza, Egypt

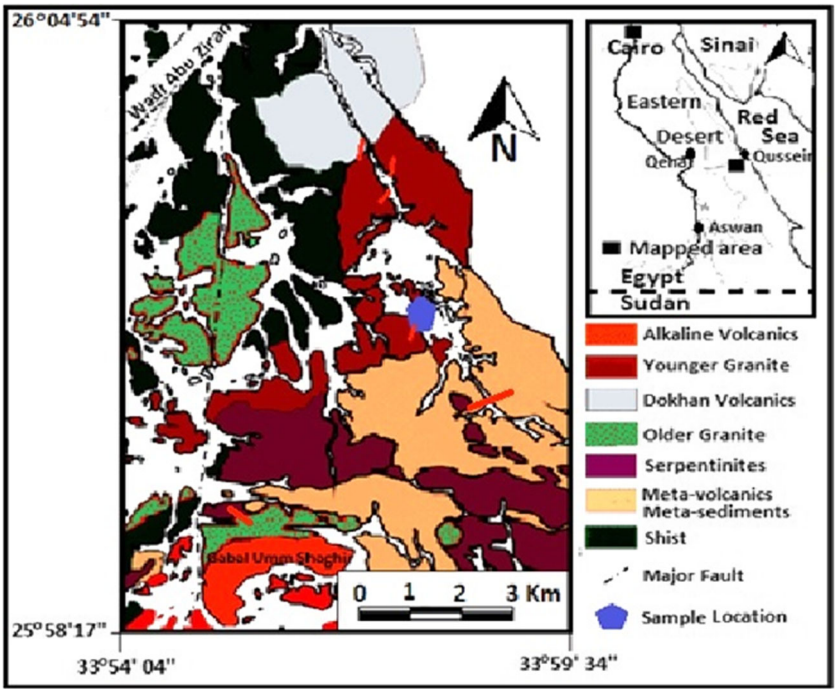

Fig. 1 Geological Map of Gabal Umm Shaghir Area [13]

The area is occupied by Precambrian basement rocks represented by; buff to pink younger granites; volcanic rocks, mainly basalts and andesites; older grey granites; metavolcanics and metasediments [11]. The area is dissected by younger Paleozoic alkaline dykes, trend NE-SW and are considered to be an offshoot from Gabal Umm Shaghir trachytic plug, occupying the southwest corner of the mapped area [12], Fig. 1. The present allanite is recorded as a constituent mineral in the qz-trachytic dykes, cut through the surrounding country buff to pink granitic rocks.

The alkaline rocks in Egypt were classified into three main types: alkali granites, syenites and related types and the late alkaline volcanics, include volcanic plugs, ring dykes and dykes [11]. Gharib and Obeid [12], considered

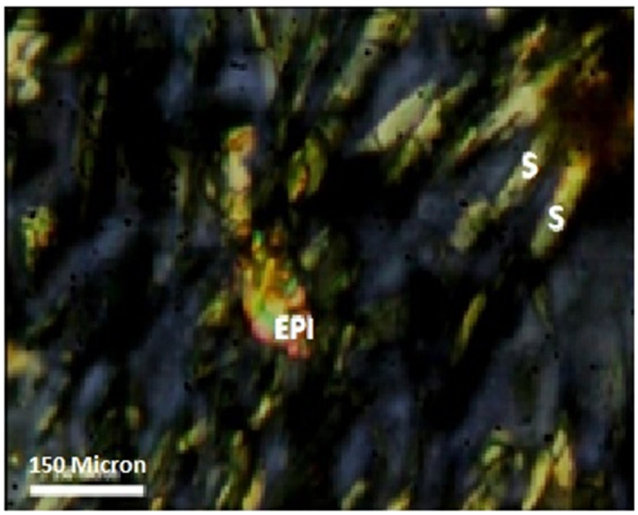

Fig. 2 Photomicrograph showing epidote (EPI) and sanidine (S) crystals arranged in preferred orientation, with the flow of the groundmass giving rise to directive texture

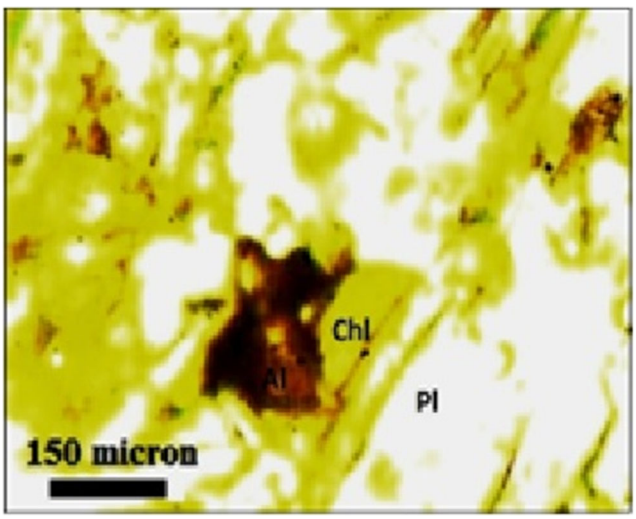

Fig. 3 Photomicrograph showing pale brown prismatic allanite crystal (Al) in contact with chlorite (Chl) and plagioclase (Pl)

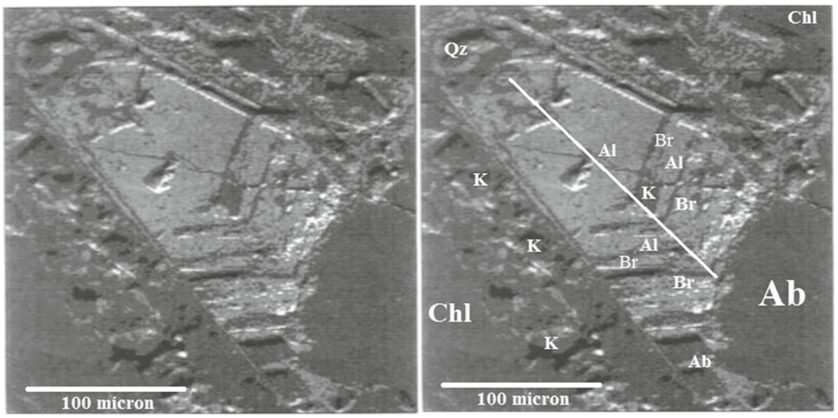

Fig. 4 Back scattered electron image showing the allanite - britholite crystal is surrounded by albite (Ab), chlorite (Chl), kaoline (K) and quartz (Qz). The straight line (in the right side) represents a plane of symmetry dividing the crystal into two identical divisions

the Paleozoic trachytic plugs at Umm Shaghir as highly fractionated quartz trachyte evolved at extensional tectonic setting. Shalaby et al. [14] studied the trachyric rocks at Gabal Abu Hibban to the southwest of Qusseir city and concluded that these rocks were evolved within continental plate tectonic regime, and their parental melts were subjected to assimilation fractional crystallization processes.

The present work aims to study the mineralogical and chemical characteristics for both allanite and britholite mineral phases, in order to determine their genesis and the genetic relations between the two REEs-silicate minerals.

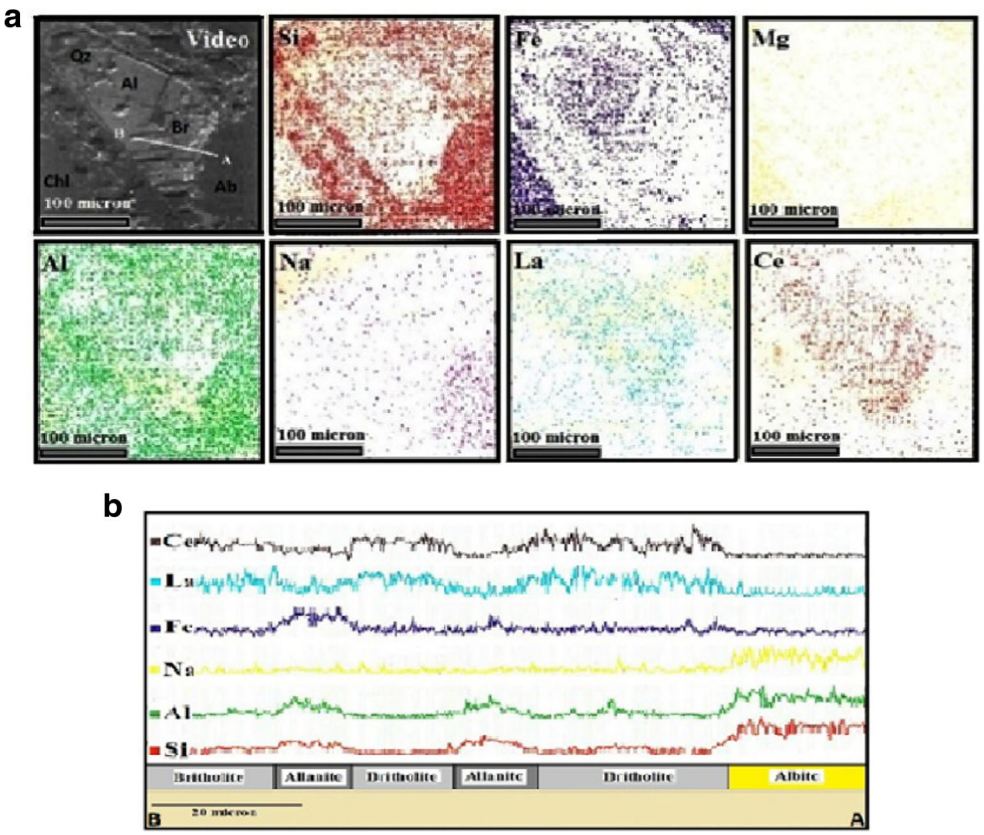

Fig. 5 **a** Elemental maps showing the distribution of Si, Fe, Mg, Al, Na, La and Ce in albite (Ab), Chlorite (Chl), quartz (Qz), allanite (Al) and britholite (Br). **b** Cross-section along A-B (in Fig. 5A) showing the relative concentration's frequencies of the selected elements between albite, britholite and allanite

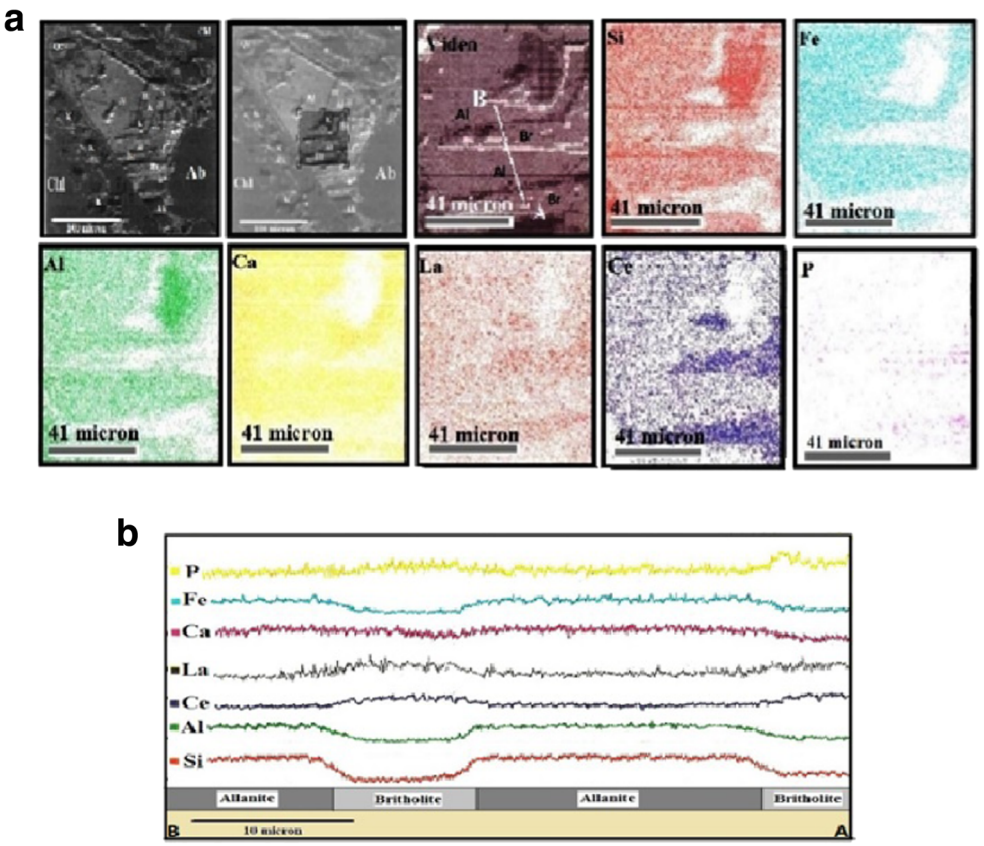

Fig. 6 **a** Zooming window on the allanite (Al) – britholite (Br) contacts, showing the distribution of Si, Fe, Al, Ca, La, Ce and P. **b** Cross-section along A-B (in Fig. 6a) showing the relative concentration's frequencies of the selected elements between britholite and allanite

2 Materials and Methods

Ten quantitative point analyses for both allanite and britholite mineral phases were done, using Cameca SX-50 electron microprobe. Concentrations of REEs were established at 25KeV with beam current of 50nA, Ce, La and Y readings based on Lα-line emissions, Nd and Sm readings collected on Lβ and Th on Mα-line emissions. All others were collected on Kα-lines. Angle was set at 40.5 degrees.

Back scattered electron images (BSE) and elemental maps for selected nine elements (Si, Al, Ca, Mg, Fe, Na, P, La and Ce), were done using energy dispersion (EDS) unit.

3 Results and Discussion

Petrographically, the host rock is fine grained, brownish gray quartz trachyte. It composed mainly of porphyritic sanidine and albite laths held together with quenched fine grained matrix, the mafic constituents represent about 15% of the total rock volume and are mainly aegerine augite, with less frequent biotite and sodic amphibole, usually altered to chlorite. Accessory minerals are zircon, epidote, apatite and allanite. The secondary minerals are carbonates, iron oxides and clay minerals. Sericitization and Kaolinization are the main alteration processes affecting the feldspar minerals. The size of the phenocrysts varies from 0.3 mm to 5 mm in length and from 0.08 to 1.0 mm in width. The quenched groundmass exhibits the characteristic flow or directive texture, as the crystals are oriented according to the flow of the parent magma, Fig. 2.

The present allanite crystal, in thin section, is pale brown, prismatic to tabular in form, pleochroice from pale brown to reddish (orange) brown, Fig. 3. In back scattered electron image (BSE), the present crystal is about 0.25 mm in length and 0.10 mm in width, the crystal encloses two mineral phases; allanite phase occupies the main bulk of the crystal, and the britholite phase, exits in the form of transversal spine-shaped lamellae, each lamella penetrates inside the allanite phase, the maximum thickness of each lamella reaches up to 10 microns at the crystal rim, and decreases gradually, inward, from the rim to the core, till it becomes tapered at its end. The britholite lamellae are bent (broken) along a line of symmetry, dividing the crystal into two identical divisions, forming an interesting fish bone-like texture Fig. 4.

The allanite side of the crystal is homogenous in tone and brightness, while the britholite lamellae exhibit various tones from light grey to dark grey, reflecting variations in

Table 1 Chemical composition and the calculated structural formula for allanite and britholite

	Allanite-Ce							Britholite-Ce				
	1	2	3	4	5	6	Average	7	8	9	10	Average
SiO_2	33.32	33.41	32.88	31.88	32.18	31.99	32.61	21.53	19.61	20.74	19.31	20.30
TiO_2	0.84	0.92	0.41	0.00	0.00	0.00	0.36	0.56	0.00	0.00	0.00	0.14
Al_2O_3	16.98	17.70	17.10	17.77	16.11	16.85	17.09	2.56	2.07	2.56	0.00	1.80
FeO	7.98	7.67	9.47	10.92	8.25	9.45	8.96	1.75	2.41	2.23	2.17	2.14
Fe_2O_3	6.50	5.60	4.81	2.41	4.83	3.95	4.68	0.00	0.00	0.00	0.00	0.00
MnO	0.08	0.00	0.00	0.00	0.00	0.00	0.01	0.00	0.00	0.00	0.00	0.00
MgO	0.81	0.79	0.68	0.00	0.62	0.00	0.48	0.89	0.00	1.39	0.00	0.57
CaO	13.83	14.22	12.39	11.20	12.67	12.36	12.78	15.14	12.45	12.62	12.73	13.24
Na_2O	0.00	0.00	0.00	0.00	0.00	0.00	0.00	0.00	0.00	0.00	0.00	0.00
K_2O	0.00	0.00	0.00	0.00	0.00	0.00	0.00	0.00	0.52	0.19	0.58	0.32
P_2O_5	0.00	0.00	0.00	0.00	0.00	0.00	0.00	3.97	3.54	3.50	3.68	3.67
La_2O_3	5.08	4.44	5.38	6.56	6.04	5.82	5.55	8.97	13.50	10.46	11.45	11.10
Ce_2O_3	9.65	9.15	10.15	10.65	10.87	11.36	10.31	25.97	24.76	28.60	26.81	26.54
Nd_2O_3	3.39	4.38	3.52	5.45	4.86	4.26	4.31	10.01	8.80	10.09	11.56	10.12
Sm_2O_3	0.48	0.51	0.48	0.76	0.91	0.91	0.68	2.10	1.99	2.33	2.37	2.20
Y_2O_3	1.06	1.21	2.73	2.40	2.66	3.05	2.19	6.55	9.11	5.29	9.34	7.57
ThO_2	0.00	0.00	0.00	0.00	0.00	0.00	0.00	0.00	1.24	0.00	0.00	0.31
Structural formula*												
Si^{4+}	3.00	2.99	3.00	2.98	3.00	2.98	2.99	2.53	2.45	2.52	2.46	2.49
Ti^{4+}	0.06	0.06	0.03	0.00	0.00	0.00	0.02	0.05	0.00	0.00	0.00	0.01
Al^{3+}	1.80	1.87	1.84	1.96	1.77	1.85	1.85	0.36	0.30	0.37	0.00	0.26
Fe^{2+}	0.60	0.57	0.72	0.85	0.64	0.74	0.69	0.18	0.25	0.23	0.23	0.22
Fe^{3+}	0.44	0.38	0.33	0.17	0.34	0.28	0.32	0.00	0.00	0.00	0.00	0.00
Mn^{2+}	0.01	0.00	0.00	0.00	0.00	0.00	0.00	0.00	0.00	0.00	0.00	0.00
Mg^{2+}	0.11	0.11	0.09	0.00	0.09	0.00	0.07	0.16	0.00	0.25	0.00	0.10
Ca^{2+}	1.33	1.36	1.21	1.12	1.26	1.24	1.25	1.90	1.66	1.64	1.74	1.73
Na^{+}	0.00	0.00	0.00	0.00	0.00	0.00	0.00	0.00	0.00	0.00	0.00	0.00
K^{+}	0.00	0.00	0.00	0.00	0.00	0.00	0.00	0.00	0.09	0.03	0.09	0.05
P^{5+}	0.00	0.00	0.00	0.00	0.00	0.00	0.00	0.40	0.38	0.37	0.40	0.39
La^{3+}	0.17	0.15	0.18	0.23	0.21	0.20	0.19	0.39	0.62	0.47	0.54	0.50
Ce^{3+}	0.32	0.30	0.34	0.36	0.37	0.39	0.35	1.12	1.13	1.27	1.25	1.19
Nd^{3+}	0.11	0.14	0.11	0.18	0.16	0.14	0.14	0.42	0.39	0.44	0.53	0.44
Sm^{3+}	0.01	0.02	0.02	0.02	0.03	0.03	0.02	0.09	0.09	0.10	0.11	0.10
Y^{3+}	0.05	0.06	0.13	0.12	0.13	0.15	0.11	0.41	0.60	0.34	0.64	0.50
Th^{4+}	0.00	0.00	0.00	0.00	0.00	0.00	0.00	0.00	0.04	0.00	0.00	0.01

*The structural formulas for both allanite and britholite are calculated on the basis of 12.5(O^{2-}), and total of 8 cations

their chemical compositions. The allanite - britholite crystal is surrounded by albite, chlorite, kaoline and very fine grained quartz (ca. 0.03 mm in length), Fig. 4.

3.1 Elemental mapping

Seven elements, (Si, Fe, Mg, Al, Na, La and Ce), were selected for elemental mapping, Fig. 5a, in order to monitor their distribution and concentrations in the different mineral phases, existing in the examined field, (albite, chlorite, kaoline, allanite and britholite). Silica and alumina are concentrated essentially in albite, and kaoline and are less frequent in allanite and chlorite, britholite is the least phase contains Si and Al. Na and Mg are restricted to albite and chlorite respectively. Fe is concentrated, essentially, in chlorite and is less frequent in allanite, and is nearly absent in britholite and albite. The LRREs; La and Ce are concentrated in both allanite

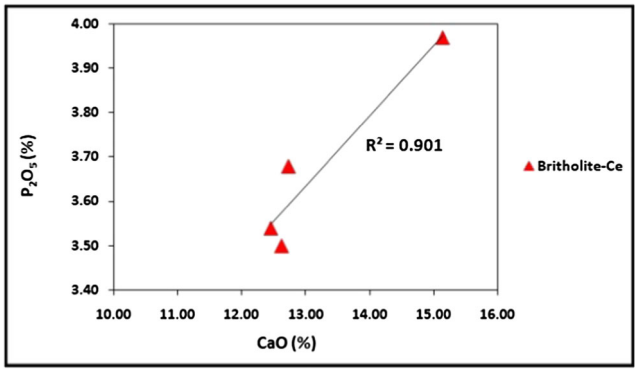

Fig. 7 Coherent coupled enrichment for CaO (%) and P_2O_5 (%) in britholite

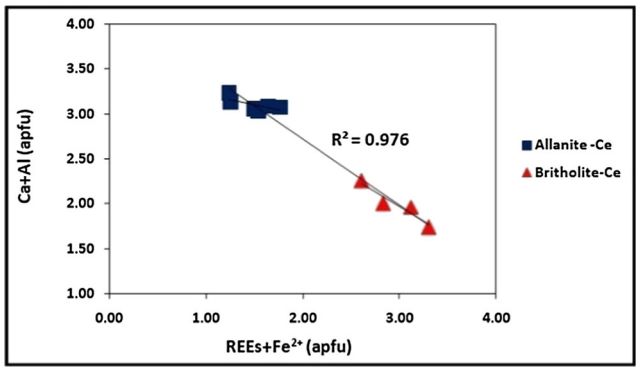

Fig. 9 Substitution between $REEs^{3+} + Fe^{2+}$ (apfu) and $Ca^{2+} + Al^{3+}$ (apfu). Wood and Ricketts, (2000) [19]

and britholite mineral phases; with more concentrations in britholite. The cross section A-B, Fig. 5b, illustrates the relative concentration's frequencies of the selected elements between albite, britholite and allanite.

More detailed elemental mapping were done through establishing a zooming or magnification window, focused on the britholite – allanite contacts, Fig, 6a. It is clear that, allanite is more enriched in Si, Al, Ca and Fe and depleted in La, Ce and P than britholite. The relative concentration frequencies of elements between the two minerals are shown, along the line A-B, in Fig. 6b, it is also clear that, the contacts between the two minerals are gradational, as investigated from the gentle slopes of the elements frequencies at the contacts between the two minerals.

3.2 Chemical composition

The electron microprobe point analyses and the calculated structural formula are listed in Table 1. The structural formulas for both allanite and britholite are calculated on the basis of 12.5 O, (12(O) + 1(OH)), and total of 8 cations. The Fe^{2+}/Fe^{3+} is adjusted until the total number of positive charges equals 25 to balance 12.5 effective O ions**,** and consequently, the FeO/Fe_2O_3 is amended.

The present chemical analyses shows that, the Ce content predominate over the other REEs in both allanite (average $Ce_2O_3\% = 10.31$) and britholite (average $Ce_2O_3\% = 26.54$), so, they could be identified as allanite-Ce and britholite-Ce.

Allanite is more enriched in SiO_2, Al_2O_3 and total iron than britholite, while the latter is more enriched in P_2O_5 and the $\Sigma REES_2O_3$. In allanite, The $SiO_2\%$ ranges from 31.88 to 33.41 with an average of 32.61%, CaO% varies from 11.20 to 14.22 with an average of 12.78%, $Al_2O_3\%$ varies from 16.11 to 17.77 with an average of 17.09%, The averages of FeO% and $Fe_2O_3\%$ are 8.96 and 4.68 respectively. The $\Sigma REES_2O_3$ varies from 18.48% to 23.42

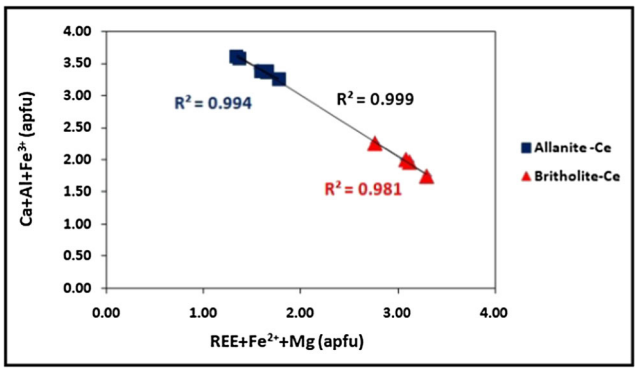

Fig. 8 Relation between $REEs^{3+} + Fe^{2+} + Mg^{2+}$ (apfu) versus $Ca^{2+} + Al^{3+} + Fe^{3+}$ (apfu). Wood and Ricketts, (2000) [19]. The negative trends, with high coefficient of determination values, demonstrate substitution between $REEs^{3+} + Fe^{2+} + Mg^{2+}$ (apfu) and $Ca^{2+} + Al^{3+} + Fe^{3}$ (apfu) from allanite to britholite

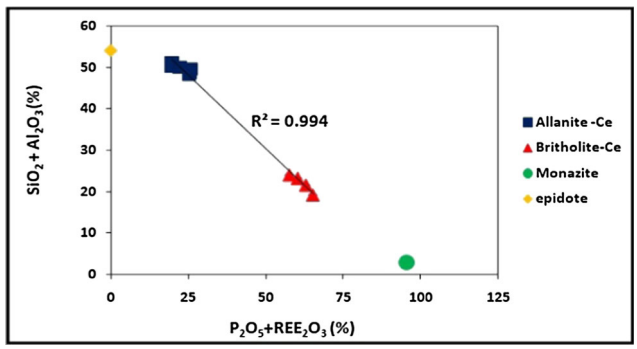

Fig. 10 Relation between $P_2O_5\% + REES_2O_3\%$ and $SiO_2\% + Al_2O_3\%$, for both present allanite and britholite phases, compared with epidote and monazite phases, epidote data are after Ahijado et al. [21] and cited from Armbruster et al. [1], monazite data are after Papunen and Lindsjö [22]. The relation illustrates a coupled substitution between $P_2O_5\% + REES_2O_3\%$ (britholite component) for $SiO_2\% + Al_2O_3\%$ (allanite component). The continuation of substitution processes may reaches to formation of monazite phase

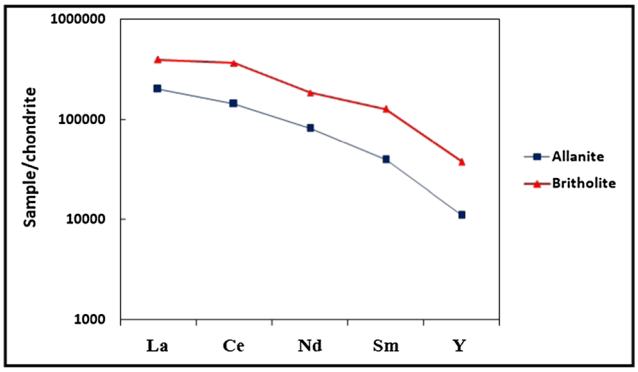

Fig. 11 The average chondrite-normalized rare- earth-elements and Y patterns ($REEs_N$ and Y_N) for both allanite and britholite, (normalization values are after McDonough and Sun [23])

% with an average of 20.84%, Y_2O_3% varies from 1.06 to 3.05 with an average 2.16%.

In britholite, SiO_2 % varies from 19.31 to 21.53 , CaO % ranges from 12.45 to 15.14 with an average of 13.24, P_2O_5% varies from 3.50 to 3.97 with an average of 3.67%, the $\Sigma REEs_2O_3$ varies from 47.05% to 52.19% with an average of 49.94%, Y_2O_3% ranges from 5.29 to 9.34 with an average 7.57%.

The thorium and Uranium contents are below the detection limit in allanite and britholite except for one analysis in britholite (ThO_2 = 1.24%), this may exclude the probability of metamictization process [15, 16]. The absence of U in allanite is encountered in some studies e.g. Suzuki et al. [17] and Hoshino et al. [18].

The structural formula of allanite is $(Ca^{2+})_{1.00}$ $(Ce^{3+}_{0.34}, La^{3+}_{0.19}, Nd^{3+}_{0.14}, Sm^{3+}_{0.02}, Y^{3+}_{0.11}, Ca^{2+}_{0.25})_{1.05}$ $(Mg^{2+}_{0.07}, Fe^{2+}_{0.69}, Fe^{3+}_{0.19})_{0.95}$ $(Ti^{4+}_{0.02}, Fe^{3+}_{0.13}, Al^{3+}_{0.85})_{1.00}$ $(Al^{3+})_{1.00}$ $(Si^{4+})_{2.99}$ $(O^{2-})_{12.5}$. The structural formula of britholite is $(Ca^{2+}_{1.73}, K^{+}_{0.05,} Mg^{2+}_{0.10}, Fe^{2+}_{0.22}, Ti^{4+}_{0.01,} Al^{3+}_{0.14,} La^{3+}_{0.50}, Ce^{3+}_{1.19}, Nd^{3+}_{0.44}, Sm^{3+}_{0.10}, Y^{3+}_{0.50,} Th^{4+}_{0.01})_{5.00}$ $(Al^{3+}_{0.12}, P^{5+}_{0.39}, Si^{4+}_{2.49})_{3.00}$ $(O^{2})_{12.5}$.

The most striking feature in the present allanite and britholite mineral phases is the coherent inter-element relations either positively (couple enrichment) or negatively (substitution). In britholite, The P_2O_5 is coupled with the increasing of CaO contents, with a high coefficient of determination value (R^2 = 0.90), Fig. 7, pointing out to a possible same source of enrichment (apatite).

Wood and Ricketts [19] suggested two coupled substitution relationships in allanite, which are; $REEs^{3+}$ + Fe^{2+} + Mg^{2+} Ca^{2+} + Al^{3+} + Fe^{3+} and $REEs^{3+}$ + $Fe^{2+}Ca^{2+}$ + Al^{3+}, (all cations are atom per formula unit (apfu)) Figs. 8 and 9. Figure 8, demonstrates the substitution between $REEs^{3+}$ + Fe^{2+} + Mg^{2+} Ca^{2+} + Al^{3+}+ Fe^{3+} for both allanite and britholite, the two minerals attain high coefficient of determination values (R^2 = 0.994 and 0.981, respectively), while the overall coefficient of determination value for the both minerals together (R^2 =0.99). This means that, there is a coherent substitution processes continued through allanite - britholite mineralizing phases. The same conclusion is also obtained from substitution processes involving $REEs^{3+}$ + Fe^{2+} Ca^{2+} + Al^{3+}, Fig. 9.

The relation between P_2O_5% +$REEs_2O_3$% and SiO_2% + Al_2O_3% shows a perfect negative linear relation, expressed by high coefficient of determination value (R^2 = 0.992), as P_2O_5 and $REEs_2O_3$ (britholite component) increase with the decrease of SiO_2+Al_2O_3 (allanite component). Such substitution illustrates a major role of phosphorous – rare earth elements bearing fluids in the formation of britholite. The continuation of such substitution may reaches to monazite phase [20], Fig. 10. This denotes that, the britholite is paragenetically formed later on, as a result of reaction between phosphorous-REEs bearing fluids and the pre-existed allanite crystal. The reaction resulted in formation of britholite as a result of hydrothermal alteration of allanite, the reaction affected a very narrow zone lining and surrounding the cleavage planes, reached up to 10 microns in width, each zone represents a britholite lamella, as shown in Fig. 6a. The reaction processes involved, essentially, substitution of P_2O_5 and $REEs_2O_3$ for Al_2O_3 and SiO_2.

The average chondrite-normalized rare- earth-elements and Y patterns ($REEs_N$ and Y_N) for both allanite and britholite, are presented in Fig. 11. The resulted two patterns are smooth and relatively parallel from La_N to Y_N, however, a faint Nd_N negative anomaly (depletion) exists in britholite pattern. It is also clear that, the two mineral phases are enriched in LREEs with gradual decreasing in normalized concentrations from La_N to Sm_N. The $REEs_N$ pattern of allanite is, relatively, more differentiated than that of britholite, as the La_N/Sm_N is 5.08 and 3.10 for allanite and britholite respectively, Fig. 11.

4 Conclusion

- Two rare earth elements bearing silicate minerals, namely allanite and britholite, are encountered coexisting in a single crystal in a quartz trachyte hosting rock.
- The allanite phase is a constituent mineral, exists as well defined crystal of about 0.25 mm in length and 0.10 mm in width, The average structural formula based on 8 cations is: $(Ca^{2+})_{1.00}$ $(Ce^{3+}_{0.34}, La^{3+}_{0.19}, Nd^{3+}_{0.14}, Sm^{3+}_{0.02}, Y^{3+}_{0.11}, Ca^{2+}_{0.25})_{1.05}$ $(Mg^{2+}_{0.07}, Fe^{2+}_{0.69}, Fe^{3+}_{0.19})_{0.95}$ $(Ti^{4+}_{0.02}, Fe^{3+}_{0.13}, Al^{3+}_{0.85})_{1.00}$ $(Al^{3+})_{1.00}$ $(Si^{4+})_{2.99}$ $(O^{2-})_{12.5}$.
- The allanite exhibited a narrow range in chemical composition, as indicated from the very close or even clustered inter-element(s) plotting.

- A secondary britholite mineral phase, exits, intergrown, inside the allanite crystal in the form of transversal spine-shaped lamellae. The average structural formula based on 8 cations is: $(Ca^{2+}_{1.73}, K^{+}_{0.05,} Mg^{2+}_{0.10}, Fe^{2+}_{0.22}, Ti^{4+}_{0.01,} Al^{3+}_{0.14,} La^{3+}_{0.50}, Ce^{3+}_{1.19}, Nd^{3+}_{0.44}, Sm^{3+}_{0.10}, Y^{3+}_{0.50,} Th^{4+}_{0.01})_{5.00}$ $(Al^{3+}_{0.12}, P^{5+}_{0.39}, Si^{4+}_{2.49})_{3.00}$ $(O^{2})_{12.5}$.
- The embayment of the britholite lamellae started from the rim to the core, and is controlled by a set of parallel planes of weakness (cleavage).
- The britholite exhibited, a relatively, more wide range of chemical variations, but such variations are far from random, the inter-element variation diagrams exhibited certain trends pointing out to either inter element coupled enrichment or substitution.
- The present britholite - allanite mineral phases, resulted from REEs + P enriched hydrothermal solutions, undergone percolation and attacking the allanite crystal along cleavage planes. The reaction between allanite crystal and the percolating fluids affected a very narrow zone; reaches up to 10 microns in width, each zone represent a britholite lamella. The reaction processes involved, essentially, substitution of P_2O_5 and $REEs_2O_3$ for Al_2O_3 and SiO_2.
- The reaction between allanite and the hydrothermal solutions, affected restricted zones, and this may be due to sudden decrease in the fluid temperature resulted in ceasing of alteration processes. However, the reaction mechanism is very complicated, as it depends on many parameters such as, the nature and the chemical composition of the hydrothermal solution, temperature, pressure and the partitioning of the REEs and P between allanite and the hydrothermal solution.

References

1. Armbruster T, Bonazzi P, Akasaka M, Bermanec V, Chopin C, Gieré R, Heuss-Assbichler S, Liebscher A, Menchetti S, Pan Y, Pasero M (2006) Recommended nomenclature of epidote-group minerals. Eur J Mineral 18:551–567
2. Levinson AA (1966) A system of nomenclature for rare-earth minerals. Am Mineral 51:152–158
3. Nickel EH, Mandarino JA (1987) Procedures involving the IMA commission on New Minerals and Mineral Names, and guidelines on mineral nomenclature. Can Mineral 25:353–377
4. Gay P (1957) An X-ray investigation of some rare earth sihcates: cerite, lessingite, beckelite, britholite and stillwellite. Mineral Mag 31:455–468
5. Pasero M, Kampf AR, Ferraris C, Pekov IV, Rakovan J, White TJ (2010) Nomenclature of the apatite supergroup minerals. Eur J Mineral 22:163–179
6. Mariano AN (1989) Economic geology of rare earth elements. In: Lipin BR, McKay GA (eds) Geochemistry and Mineralogy of Rare Earth Elements. Rev. Mineral, vol 21, pp 309–337
7. Gindy AR (1961) Allanite from Wadi El Gemal area, Eastern Desert of Egypt, and its radioactivity. Am Mineral 46:985–93
8. Asran AMH, El-Mansi MM, Ibrahim ME, Abdel Ghani IM (2013) Pegmatites of Gabal El Urf, Central Eastern Desert, Egypt. The Seventh International Conference On The Geology Of Africa, Assiut, Egypt, IV-1 - IV-22
9. Ragab AA, Assran HM (2007) Mineralogy and geochemistry of rare Metals-Bearing pegmatite from South Eastern Desert, Egypt. The Fifth International Conference On The Geology of Africa 1:95–129
10. Saleh GM (2007) Geology and rare-earth element geochemistry of highly evolved, molybdenite-bearing granitic plutons, Southeastern Desert, Egypt. Chin J Geochem 26(4):333–344
11. Akaad MK, El-Ramly MF (1961) The nepheline syenite ring complex of Gabal Abu Khruq, South Eastern Desert of Egypt. Geol. Surv. Egypt. Paper No. 14
12. Gharib ME, Obeid MA (2012) Paleozoic alkaline volcanism: geochemistry and petrogenesis of Um Khors and Um Shaghir trachytes of the Central Eastern Desert. Egypt Arab J Geosci 5:53–71
13. El-Ramly MF (1972) A new geological map for the basement rocks in the Eastern and Southwestern Desert of Egypt. Ann Geol Surv Egypt 2:1–18
14. Shalaby BNA, El-Maghraby MS, Mashaly AO, Salem AKA (2017) Geochemical characterization of Trachytic Rocks At Gabal Abu Hibban, Central Eastern Desert, Egypt, And Their Suitability As A Flux In Ceramic Industry. Res J Appl Sci 12(2):242–253
15. Ercit TS (2002) The mess that is "allanite". Can Mineral 40:1411–1419
16. Cobic A, Bermanec V, Tomasic N (2010) The hydrothermal recrystallization of metamict Allanite-(Ce). Can Mineral 48:513–521
17. Suzuki K, Adachi M, Yamamoto K (1990) Possible effects of grain-boundary REE on the REE distribution in felsic melts derived by partial melting. Geochem J 24:57–74
18. Hoshino M, Kimata M, Nishida N, Kyono A, Shimizu M, Takizawa S (2005) The chemistry of allanite from the Daibosatsu Pass, Yamanashi, Japan. Mineral Mag 69(4):403–423
19. Wood SA, Ricketts A (2000) Allanite-(ce) from the Eocene Casto granite, Idaho: response to hydrothermal alteration. Can Mineral 38:81–100
20. Hirtopanu P, Andersen JC, Fairhurst RJ, Jakab G (2013) Allanite-(Ce) And its associations, from the ditrau alkaline intrusive massif, East Carpathians, Romania. The publishing house of the Romanian academy, Series B 15(1):59–74
21. Ahijado A, Casillas R, Nagy G, Fernández C (2005) Sr-rich minerals in a carbonatite skarn, Fuerteventura, Canary Islands (Spain). Mineral Petrol 84:107–127
22. Papunen H, Lindsjö O (1972) Apatite, monazite and allanite; three rare earth minerals from korsnäs, Finland. Bull Geol Soc Finl 44:123–129
23. McDonough WF, Sun SS (1995) Composition of the earth. Chem Geol 120:223–253